Received: 29 May 2024 | Revised: 26 October 2024 | Accepted: 17 December 2024

DOI: 10.1111/bph.17445

RESEARCH ARTICLE

Characterisation of neurogenic lipolytic responses in white adipose tissue ex vivo

Kayleigh E. Goddard | Samuel J. Fountain

School of Biological Sciences, University of East Anglia, Norwich, UK

Correspondence
Samuel J. Fountain, School of Biological Sciences, University of East Anglia, Norwich Research Park, Norwich NR4 7TJ, UK.
Email: s.j.fountain@uea.ac.uk

Funding information
Biotechnology and Biological Sciences Research Council; British Heart Foundation, Grant/Award Number: PG/19/35/34389

Background and Purpose: Dysfunction of the autonomic nervous system is associated with cardiovascular dysfunction, including metabolic syndrome and obesity. Understanding mechanisms of neurogenic control of white adipose tissue is key to understanding adipose physiology and pathophysiology, though there is limited research exploring this in adipose tissue using pharmacological tools, as opposed to genetic knockout models.

Experimental Approach: Inguinal white adipose tissue from C57BL/6J mice was used in this study. We used immunocytochemistry to determine tissue innervation and glycerol release assays to quantify lipolysis in adipose tissue and isolated adipocytes. The voltage-gated Na^+ channel opener veratridine was used to stimulate nervous activity in tissue ex vivo. The role of neurotransmitters and receptors mediating veratridine-evoked lipolysis in adipose tissue was pharmacologically characterised.

Key Results: Veratridine evoked glycerol release in white adipose tissue but not from isolated adipocytes. This release was abolished by tetrodotoxin and propranolol. Veratridine also induced noradrenaline release from white adipose tissue. Veratridine- and noradrenaline-evoked glycerol release was blocked by the β_2-adrenoceptor antagonist ICI-118551 but not by the β_1-adrenoceptor antagonist CGP 20712A. Purported β_3-adrenoceptor antagonists L-748337 and SR59230A stimulated glycerol release from tissue and from isolated adipocytes. Neither L-748337 or SR59230A antagonised veratridine-evoked glycerol release but SR59230A antagonised noradrenaline-evoked glycerol release. We exclude contributions of sensory neuropeptides and the autonomic neurotransmitters neuropeptide Y and ATP.

Conclusion and Implications: Neurogenic lipolytic responses can be measured in white adipose tissue ex vivo using veratridine to stimulate nerve activity. The lipolytic responses are mediated by β_2-adrenoceptor activation. This study provides the first evidence of neurogenic lipolysis in tissue ex vivo.

KEYWORDS
adipose, neurogenic, neurotransmitter, obesity

Abbreviations: PPADS, pyridoxal phosphate-6-azo(benzene-2,4-disulfonic acid); TTX, tetrodotoxin.

1 | INTRODUCTION

Pharmacological manipulation of white adipose tissue is a growing area of interest for the treatment of metabolic syndrome, obesity and associated cardiovascular disease (Kusminski et al., 2016). White adipose tissue is the major depot for energy storage, a critical endocrine organ, and central to regulated whole-body energy expenditure and appetite through the release of adipokines. Dysfunction of white adipose tissue increases cardiovascular risk and is associated with obesity, metabolic syndrome and ectopic deposition of fat (Kawai et al., 2021; Koenen et al., 2021). The major cellular component of white adipose tissue is the adipocyte, which sequesters excess dietary glucose and fatty acids and stores them as triglycerides. During positive energy balance, this process is stimulated by insulin, which promotes energy storage. During negative energy balance, triglycerides stored within adipocyte lipid droplets are subject to hydrolysis, freeing energy in the form of fatty acids and glycerol (lipolysis). Adipose tissue can also increase its energy buffering capacity under physiological conditions through hypertrophic and hyperplastic mechanisms.

In addition to hormonal regulation, the function of white adipose tissue is also under regulation by both the autonomic and sensory arms of the peripheral nervous system (Bartness et al., 2014; Wang et al., 2022). In animal models, local sympathetic denervation leads to the expansion of white adipose tissue (Bowers et al., 2004). Such observations are believed to be caused by the removal of sympathetic adrenergic activity, working primarily through β-adrenoceptor activation stimulating lipolysis in adipocytes, though information at the level of adipose tissue is missing. In addition, a paradoxical situation arises in metabolic syndrome and obesity, where white adipose tissue expands and is maintained despite increased sympathetic nervous activity (Esler et al., 2018). The precise mechanisms underlying the development of a refractory response to catecholamines in white adipose tissue during increased sympathetic outflow in metabolic syndrome and obesity remain unclear, but down-regulation of β-adrenoceptors and inflammation have been suggested (Mowers et al., 2013; Valentine et al., 2022). Further mechanistic understanding of how the peripheral nervous system controls white adipose tissue and the development of appropriate models is therefore required.

Although numerous studies have investigated the actions of neurotransmitters (Ali et al., 2018a) and hormones on adipocytes, freshly isolated from either tissue or adipocyte-like cell lines, there are limited studies that examine the consequence of increased nervous activity in white adipose tissue ex vivo. This is critical to better understand the role of the peripheral nervous system in white adipose tissue physiology and to understand the action of pharmacological agents intended to manipulate adipocyte function in the context of adipose tissue, which contains multiple cell types. Here, we take a novel approach using the steroid alkaloid veratridine to stimulate nervous activity in white adipose tissue ex vivo and explore the role of sympathetic and sensory neurotransmitters in regulating lipolysis.

What is already known

- Dysfunction of the autonomic nervous syndrome is associated with cardiovascular disease and obesity.

What does this study add

- Veratridine is identified as an experimentally useful tool to study neurogenic responses in adipose tissue ex vivo.

What is the clinical significance

- The results provide opportunity for target validation in cardiovascular disease and obesity.

2 | METHODS

2.1 | Animals

All animal care and experimental procedures complied with the UK Animals (Scientific Procedures) Act 1986 and were approved by the Animal Welfare & Ethical Review Board of the University of East Anglia, UK. Animal studies are reported in compliance with the ARRIVE guidelines (Percie du Sert et al., 2020) and with the recommendations made by the *British Journal of Pharmacology* (Lilley et al., 2020).

Male mice were used in this study due to reported sexual dimorphic metabolic response in C57BL/6J mice (Casimiro et al., 2021) and the influence of oestradiol cycling on white adipose tissue physiology in mice (Saavedra-Peña et al., 2023). However, female C57BL/6J mice were used in one set of experiments. C57BL/6J mice were used as a model due to their use in exploring mechanisms of cardiovascular disease and potential for genetic manipulation in follow-on studies (Doevendans et al., 1998).

The mice used in the studies described here were provided by the animal facility of the University of East Anglia. Male C57BL/6J mice (8–10 weeks old) weighing 20–30 g were used in the majority of work in this study. However, non-pregnant female C57BL/6J mice (8–10 weeks old) were used in one set of experiments, as described later.

Mice were housed in a specific pathogen-free, with *Staphylococcus aureus* and *Klebsiella* exclusion, barriered facility with the Disease Modelling Unit, University of East Anglia. A maximum of five adult mice per cage were housed in Techniplast blue slimline cages (Type 1284). Cages contained PG2 bedding (International Product Supplies Ltd), rodent rolls and aspen wood chew blocks (LB Biotechnology). Each cage contained a red polycarbonate mouse hut and tunnel. All cages are prepared, sealed and then autoclaved at 121°C for 15 min.

Most mice were bred in trios (one male and two female). Light is provided on a 12/12-h cycle (7:00 AM–7:00 PM) with a dawn (6:30 AM) and dusk (7:30 PM) period where lobby lights are on for an additional 30 min. Temperature was maintained at 21 ± 2°C and humidity at 55 ± 10%. Irradiated 5LF5 rodent diet and filtered water were available ad libitum. Mice were checked daily, prior to Schedule 1 procedures, for signs of ill health. The animal facility is screened quarterly for the full Federation of European Laboratory Animal Science Associations (FELASA) list of organisms.

2.2 | Adipocyte isolation

Animals were humanely killed by CO_2 asphyxiation followed by cervical dislocation, carried out in accordance with the UK Animals (Scientific Procedures) Act 1986. Inguinal adipose tissue was subsequently removed for experimentation. Pairs of inguinal white adipose depots were dissected and rinsed in Hanks' balanced salt solution (HBSS) before mincing with a scalpel blade. HBSS contained (mM): 137 NaCl, 5.3 KCl, 1.3 $CaCl_2$, 0.4 $MgSO_4$, 1 $MgCl_2$, 0.42 Na_2HPO_4, 0.44 KH_2PO_4, 5.5 D-glucose and 4.16 $NaHCO_3$. Tissue was digested for 30 min at 37°C in 5-ml HBSS containing 40-μg·ml^{-1} DNase I (Biomatik) and 0.2-mg·ml^{-1} type 1A collagenase (Merck). The digest was gently inverted every 10 min to encourage dissociation. The digest was passed through a 100-μm cell strainer and rinsed with 50-ml HBSS before centrifugation at 50 × *g* for 4 min, at room temperature (20 – 22°C). The adipocyte 'halo' was gently removed and rinsed with either Dulbecco's modified Eagle's medium (DMEM) for glycerol assays or HBSS for total RNA extraction. Adipocytes were centrifuged again at 50 × *g* for 4 min at room temperature (20 – 22°C).

2.3 | Glycerol release assays

The assay buffer was consisted of glucose (5 mM), phenol-red free DMEM supplemented with 2% (w/v) fatty acid-free bovine serum albumin and 25-mM 4-(2-hydroxyethyl)-1-piperazineethanesulfonic acid (HEPES). For experiments involving tissue, pairs of inguinal white adipose depots were washed in HBSS and cut into approximately 10- to 15-mg pieces; 150 μl of assay buffer was added to each piece of tissue in 1.5-ml tubes. Reactions with assay buffer alone were used as blanks and subtracted from all experimental data. The amount of glycerol released was normalised to the wet mass of tissue pieces determined before experimentation. For experiments with isolated adipocytes, the number of adipocytes was not determined. Instead, 50 μl of adipocytes from a given preparation was added to each well of a 96-well plate followed by 50 μl of assay buffer. Test reactions were normalised by subtracting the amount of glycerol produced in untreated cells for a given preparation. For all glycerol assays, antagonists or vehicle controls were pre-incubated with tissue or cells for 30 min at room temperature prior to starting assays. Assays were performed at 37°C for up to 3 h in a humidified environment; a 10-μl sample was removed for quantification of free glycerol using an absorbance-based glycerol assay kit (Merck). Absorbance was determined using an Eppendorf 6131 spectrophotometer.

2.4 | Noradrenaline outflow assay

The assay buffer was comprised of low glucose (5 mM), phenol-red free DMEM supplemented with 2% (w/v) fatty acid-free bovine serum albumin and 25-mM HEPES. For experiments involving tissue, pairs of inguinal white adipose depots were washed in HBSS and cut into approximately 10- to 15-mg pieces; 150 μl of assay buffer was added to each piece of tissue in 1.5-ml tubes. At the end of experiments, 100 μl of medium was withdrawn, and **noradrenaline** was quantified by enzyme-linked immunosorbent assay (ELISA) (Abnova). Absorbance values for assay buffer alone were subtracted from all test measurements. The amount of noradrenaline was normalised to the predetermined tissue wet mass. Antagonists or vehicle controls were pre-incubated with tissue or cells for 30 min at room temperature prior to starting assays.

2.5 | Reverse transcription polymerase chain reaction (RT-PCR)

Total RNA was extracted from adipose tissue or adipocytes using Tri Reagent as previously described (Ali et al., 2018a, 2018b); 1- to 2-μg total RNA from adipocytes or 0.5- to 1-μg total RNA for adipose tissue was used for cDNA synthesis in 200-U SuperScript III (Invitrogen) with 100-ng random hexamers (Promega). Polymerase chain reaction (PCR) was performed using Taq Polymerase (Promega) with thermal cycling protocol of initial denaturation at 94°C for 90 s, then 35–40 cycles of 94°C for 30 s, 55–60°C for 30 s, 72°C for 45 s and a final extension of 72°C for 6 min. Sequences of oligonucleotide primers used are given in Table S1.

2.6 | Immunocytochemistry

The Immuno-related procedures used comply with the recommendations made by the *British Journal of Pharmacology*. Whole-mount immunocytochemistry methods applied were based upon those described by Willows et al. (2021). Briefly, adipose tissue was fixed with 4% (w/v) paraformaldehyde for 2–3 h before washing with phosphate-buffered saline (PBS) containing 1% (v/v) Triton X-100 and 10-U·ml^{-1} heparin for 6–8 h. Tissue was then blocked for 48–72 h at 4°C in blocking buffer composed of PBS containing 1% (v/v) Triton X-100, 5% (v/v) normal goat serum and 5% (v/v) bovine serum albumin. After blocking, tissue was flattened using glass slides and binder clips for 90 min at 4°C. Tissue was treated with 0.1% (w/v) Sudan black in ethanol for 20 min at room temperature to quench lipid autofluorescence, followed by washing for 8 h in PBS containing 1% (v/v) Triton X-100. Primary antibodies were diluted in blocking buffer as follows: anti-β_3-tubulin (1:500; Abcam ab41489, RRID:AB_727049) and anti-tyrosine hydroxylase (1:250; Millipore ab152, RRID:AB_390204). Primary antibodies were applied for 48 h rotating at 4°C and then washed for 8 h in PBS before application of secondary

antibodies. Triton X-100. Secondary antibodies were diluted in blocking buffer as follows: goat anti-chicken Alexa 488 (1:500; Abcam ab150173, RRID:AB_2827653) and goat anti-rabbit 647 (1:500; Invitrogen A-21245, RRID:AB_141775). Additional stains including isolectin B4 (2 $\mu g \cdot ml^{-1}$; Invitrogen I32450) and BODIPY (20 $\mu g \cdot ml^{-1}$; Invitrogen D3922) were applied during the secondary antibody step. Tissue was washed for a further 8 h in PBS before further flattening 36–72 h prior to imaging. Tissue was imaged by confocal microscopy using a Zeiss LSM 980 confocal microscope with Airyscan.

2.7 | Experimental design and analysis

The data and statistical analysis comply with the recommendations of the *British Journal of Pharmacology* on experimental design and analysis in pharmacology (Curtis et al., 2022). Mice were randomly allocated to groups. The experimenter was not blinded to treatments. Statistical analysis was performed on experimental groups containing at least five animals per group. Data were checked for normality (Shapiro–Wilk) and variance (Levene's) before one-way analysis of variance (ANOVA) with post hoc Tukey test or Welch ANOVA with Games–Howell post hoc analysis was conducted. Student's *t* tests or Mann–Whitney *U*-tests were performed for analysis between two groups. All statistical analyses were performed using OriginPro Version 2024 software from OriginLab Corporation (Northampton, MA, USA). Throughout the study, 'N' indicates the number of biological replicates and 'n' the number of technical replicates.

2.8 | Materials

Tocris Bioscience (Bristol, UK) supplied the following: BIBO3304 trifluoroacetate (Cat # 2412), BIIE 0246 hydrochloride (Cat # 7377/1), BIBN 4096 (Cat # 4561/10), A 317491 sodium salt (Cat # 6493), ω-conotoxin GVIA (Cat # 1085), KB-R7943 mesylate (Cat # 1244), CGP37157 (Cat # 1114), SR59230A hydrochloride (Cat # 1511), CGP 20712 dihydrochloride (Cat # 1024), ICI-118551 hydrochloride (Cat # 0821), L-748,337 (Cat # 2760), CP 96345 (Cat # 2893) and L-152,804 (Cat # 1382). Alomone Labs (Jerusalem, Israel) supplied the ω-conotoxin MVIIC (Cat # SNX-230) and Abcam (Cambridge, UK) supplied the following: isoprenaline hydrochloride (Cat # ab146724), veratridine (Cat # ab120279) and tetrodotoxin (TTX) citrate (Cat # ab120055). Merck Life Sciences (Darmstadt, Germany) supplied the following: nifedipine (Cat # N7634-1G), L- noradrenaline hydrochloride (Cat # 74480-100MG), cilnidipine (Cat # C1493), (±)-propranolol hydrochloride (Cat # P0884), pyridoxal phosphate-6-azo(benzene-2,4-disulfonic acid) (PPADS) tetrasodium salt hydrate (Cat # P178), suramin sodium salt (Cat # S2671), DMEM—low glucose (Cat # D4947), bovine serum albumin (Cat # A7030) and glycerol assay kit (Cat # MAK117). Thermo Fisher Scientific (MA, USA) supplied the HEPES (Cat # 11422497) and Abnova supplied the noradrenaline ELISA kit (Cat KA1891).

2.9 | Nomenclature of targets and ligands

Key protein targets and ligands in this article are hyperlinked to corresponding entries in http://www.guidetopharmacology.org and are permanently archived in the Concise Guide to PHARMACOLOGY 2023/24 (Alexander, Christopoulos, Davenport, Kelly, Mathie, Peters, Veale, Armstrong, Faccenda, Harding, Davies, et al., 2023; Alexander, Fabbro, Kelly, Mathie, Peters, Veale, Armstrong, Faccenda, Harding, Davies, Amarosi, et al., 2023; Alexander, Fabbro, Kelly, Mathie, Peters, Veale, Armstrong, Faccenda, Harding, Davies, Annett, et al., 2023; Alexander, Fabbro, Kelly, Mathie, Peters, Veale, Armstrong, Faccenda, Harding, Davies, Beuve, et al., 2023; Alexander, Kelly, Mathie, Peters, Veale, Armstrong, Buneman, Faccenda, Harding, Spedding, Cidlowski, et al., 2023; Alexander, Mathie, Peters, Veale, Striessnig, Kelly, Armstrong, Faccenda, Harding, Davies, Aldrich, et al., 2023).

3 | RESULTS

An immunocytochemical study of the inguinal fat pad in whole-mount revealed three distinct modes of innervation within the tissue (Figure 1). The first mode was is the presence of large nerve bundles tracking through the tissue, indicated by the pan-neuronal marker β-tubulin III (Figure 1a). Nerve axons were both sympathetic (positive for **tyrosine hydroxylase**), and non-sympathetic (negative for tyrosine hydroxylase; Figure 1a). The second mode was perivascular innervation. Small calibre blood vessels (2.7- to 5.2-μm diameter; N = 4, n = 118) were readily detectable through positive staining with isolectin B4 (Figure 1b). β-Tubulin III staining was not readily detectable for small calibre vessels, revealing a general lack of innervation (Figure 1b). Medium (10.1- to 30.9-μm diameter; N = 4, n = 53) (Figure 1c) and large (49.2- to 141-μm diameter; N = 7, n = 14) (Figure 1d) calibre blood vessels were not stained with isolectin B4 but were detectable via their autofluorescence. In contrast to small calibre blood vessels, medium and large blood vessels were supplied by nerves, with clear β-tubulin III-positive structures tracking along vessels (Figure 1c,d). The innervation of both medium- and large-calibre blood vessels was sympathetic, as indicated by tyrosine hydroxylase positivity, but with occasional examples of β-tubulin III-positive tyrosine hydroxylase-negative nerves (Figure 1c,d). The third mode was innervation of parenchyma, away from blood vessels, and of individual adipocytes. We observed nerve-like structures positive for β-tubulin III and tyrosine hydroxylase that tracked across adipocytes and traced routes in between adipocytes (Figure 1e). Some β-tubulin III-positive cells were found away from blood vessels (Figure 1f) and, on occasion, formed lattice-like structures around individual cells (Figure 1g). These results suggest that there is innervation of medium and large blood vessels perfusing white adipose tissue, but that some axons also project away from vascular structures and appear to innervate adipocytes by passing in close proximity and also forming lattices around individual cells.

In white adipose tissue, robust lipolytic responses were evoked by the non-selective β-adrenoceptor agonist **isoprenaline** and the

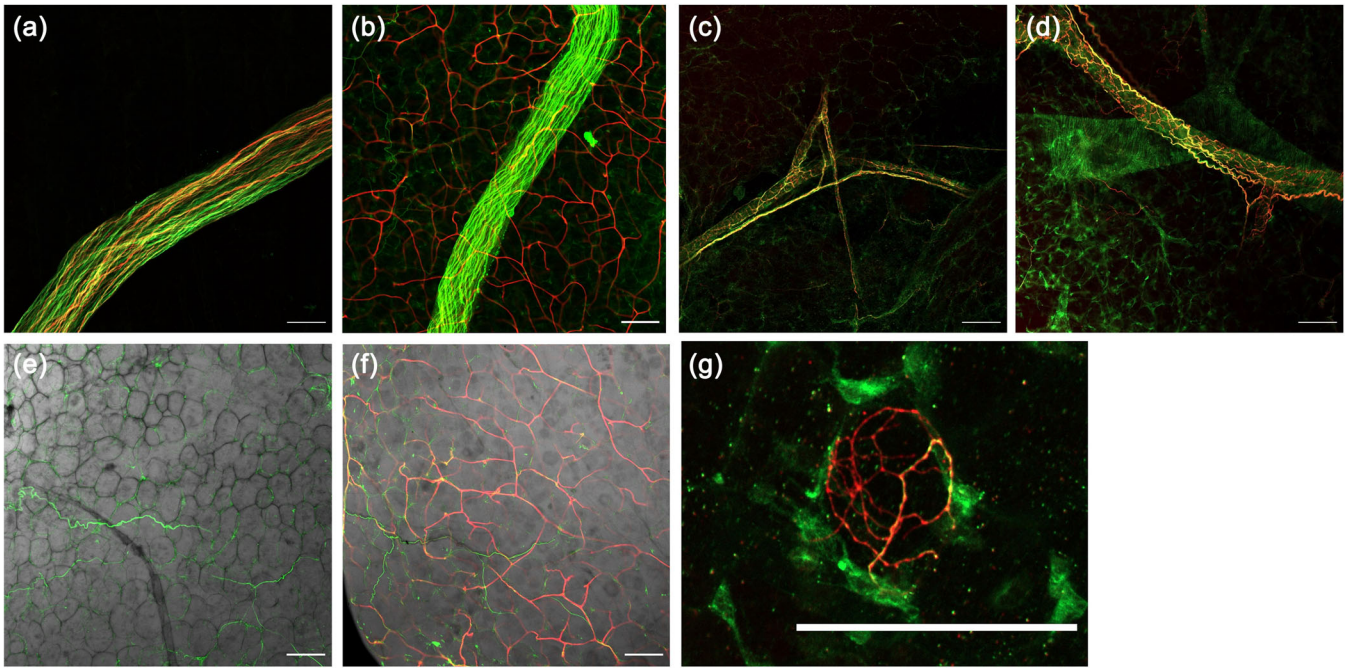

FIGURE 1 Modes of innervation in white adipose tissue. Representative whole-mount confocal microscopy images of inguinal white adipose tissue showing different types of nerve supply in the tissue.. (a) Large nerve bundles labelled with β-tubulin III (green) and tyrosine hydroxylase (red). (b) Small calibre blood vessels without innervation, labelled with isolectin B4 (red). Nerve bundle shown labelled with β-tubulin III (green). (c) Medium and (d) large blood vessels detectable by autofluorescence (green), innervated by tyrosine hydroxylase-positive (red) nerves (β-tubulin III; green). (e) Innervation (β-tubulin III; green) of adipose tissue parenchyma. Adipocytes visual in bright-field image. (f) Nerves in adipose tissue (β-tubulin III; green) not associated with blood vessels (isolectin B4; red). (g) Example of tyrosine hydroxylase (red) nerves (β-tubulin III; green) showing lattice-like structure around an individual adipocyte. Scale bars are 100 μm.

sympathetic neurotransmitter noradrenaline (Figure 2a). Noradrenaline evoked glycerol release from adipose tissue in a concentration-dependent fashion with a half-maximal concentration of 2.4 ± 1.4 μM (N = 5) (Figure 2b). The release of glycerol in response to noradrenaline was time-dependent over the 3-h period tested, significantly increasing glycerol release at 2 and 3 h compared to the basal level of glycerol release from the tissue (Figure 2c). In a strategy to evoke neurogenic responses in white adipose tissue, we employed **veratridine**, a plant natural product known to inhibit inactivation of voltage-gated Na^+ channels. Application of 100-μM veratridine stimulated robust release of glycerol from adipose tissue, to a level equivalent to the half-maximal response to noradrenaline (Figure 2d). The response to veratridine was concentration-dependent (Figure 2e) and time-dependent, significantly increasing glycerol release from 1-h exposure compared to the basal level of glycerol release from the tissue (Figure 2f). Importantly, the response to veratridine was abolished by **TTX** (Figure 2g), revealing a dependency upon **voltage-gated Na^+ channels**. TTX had no effect on basal release of glycerol in adipose tissue (Figure 2h). To explore sexual dimorphism in the responsivity to veratridine, we also undertook experiments using inguinal fat pads from female mice. In these experiments, the amount of glycerol released following stimulation with noradrenaline and veratridine was not significantly different from male mice (N = 5). The amount of glycerol released in response to noradrenaline and veratridine in female mice was also not significantly different (Figure S1).

As there is evidence that white adipocytes can express some types of voltage channels (Fedorenko et al., 2020; Zhai et al., 2020), but no reports of voltage-gated Na^+ channels, we considered it important to confirm that veratridine did not act directly on white adipocytes to stimulate glycerol release. To investigate this, we used a purified preparation of white adipocytes isolated from the inguinal fat pad. We confirmed the purity of adipocytes in this preparation by RT-PCR analysis using primer sets to identify non-adipocyte cell types known to present in white adipose tissue, often referred to as the stromal vascular fraction (SVF). The SVF markers included for the vasculature: **PDGF receptors**, smooth muscle actin, lymphatic vessel endothelial hyaluronan receptor 1 (Lyve-1), platelet endothelial cell adhesion (Pecam-1) and **CD146**; for immune cells: lymphocyte common antigen **CD45**, CD8 and **CD14**; and for neurons: β_3-tubulin. Perilipin-1 was used as an adipocyte marker. SVF and adipocyte markers were all detectable by RT-PCR using cDNA from whole adipose tissue (Figure 3a). Perilipin-1 but no SVF markers were detectable in freshly isolated adipocyte preparations (Figure 3b), confirming the purity of the adipocyte preparation. Noradrenaline elicited robust glycerol release in adipocytes, but veratridine did not (Figure 3c). These data indicate that adipocytes are not the target for veratridine in white adipose tissue, and we suggest that the target is nerves supplying the tissue (Figure 1). To this end, we probed the contribution of different neurotransmitters to the glycerol release mediated by veratridine, in white adipose tissue.

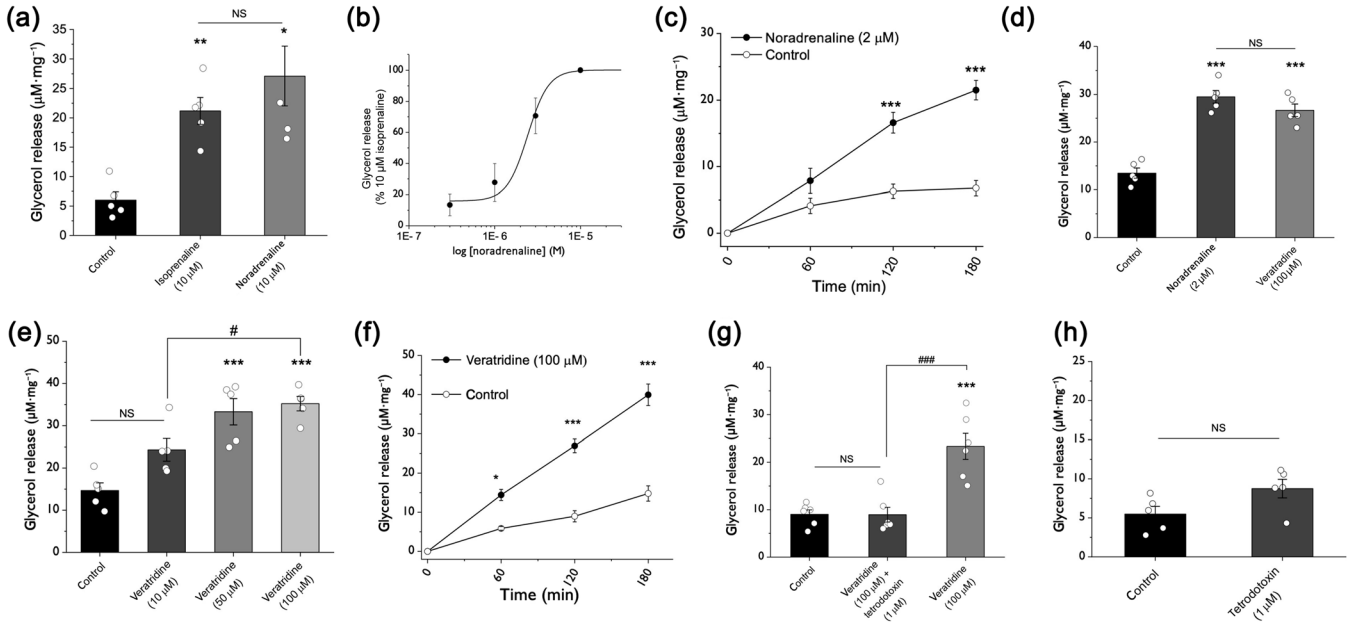

FIGURE 2 Veratridine evokes neurogenic lipolysis in white adipose tissue. (a) Adrenoceptor agonists - isoprenaline and noradrenaline - stimulate glycerol release in white adipose tissue (N = 5). (b) Concentration–response relationship for noradrenaline-evoked glycerol release (N = 5). (c) Time dependency of noradrenaline at half-maximal concentration to stimulate glycerol release over basal glycerol release (N = 5). (d) Glycerol release stimulated by veratridine compared to a half-maximal concentration of noradrenaline (N = 5). (e) Veratridine stimulates glycerol release in a concentration-dependent fashion (N = 5). (f) Time dependency of veratridine at maximal concentration to stimulate glycerol release over basal glycerol release (N = 5). (g) Tetrodotoxin abolishes veratridine-evoked glycerol release (3 h; N = 6). (h) Tetrodotoxin has no effect on basal glycerol release (N = 5). Tissue was pre-incubated with antagonists for 30 min at room temperature prior to stimulation. Glycerol released is expressed as $\mu M \cdot mg^{-1}$ wet tissue. All responses are measured after 3 h unless otherwise stated. $^{*}P < 0.05$, $^{**}P < 0.01$, $^{***}P < 0.001$, significantly different from vehicle control or between test and control groups for (c) and (f). $^{\#}P < 0.05$, $^{\#\#\#}P < 0.001$, significantly different as indicated; NS, no significance between compared groups.

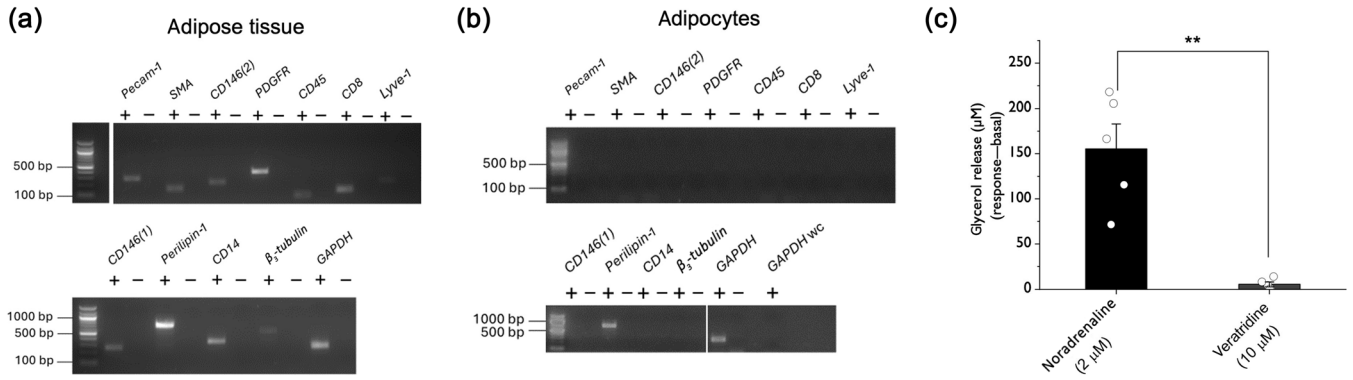

FIGURE 3 Veratridine does not stimulate glycerol release in isolated white adipocytes. RT-PCR analysis of stromal vascular fraction (SVF) markers in (a) white adipose tissue and (b) isolated white adipocytes. SVF markers—vasculature: platelet-derived growth factor receptor (PDGFR), smooth muscle actin (SMA), lymphatic vessel endothelial hyaluronan receptor 1 (Lyve-1), platelet endothelial cell adhesion (Pecam-1) and CD146; immune cells: lymphocyte common antigen, CD45, CD8 and CD14; neurons: β_3-tubulin. Perilipin-1 was used as an adipocyte marker. GADPH is positive control. (c) Glycerol release experiments in isolated white adipocytes stimulated with noradrenaline or veratridine (N = 5). Basal glycerol release measured in untreated cells is subtracted from all test measurements. $^{**}P < 0.01$. '+/−' refers to the presence or absence of reverse transcriptase. Gels are representative of three biological repeats.

We next probed some general mechanisms associated with neurotransmitter release to further understand the mechanism of veratridine action. **ω-Conotoxin GVIA**, selective for N-type **voltage-gated Ca^{2+} channels**, had no apparent effect on either veratridine-evoked glycerol release or the basal rate of glycerol release (Figure 4a). **ω-Conotoxin MVIIC**, which blocks N-type and P/Q-type voltage-gated Ca^{2+} channels, also had no obvious effect on veratridine-evoked glycerol release or the basal rate of glycerol release

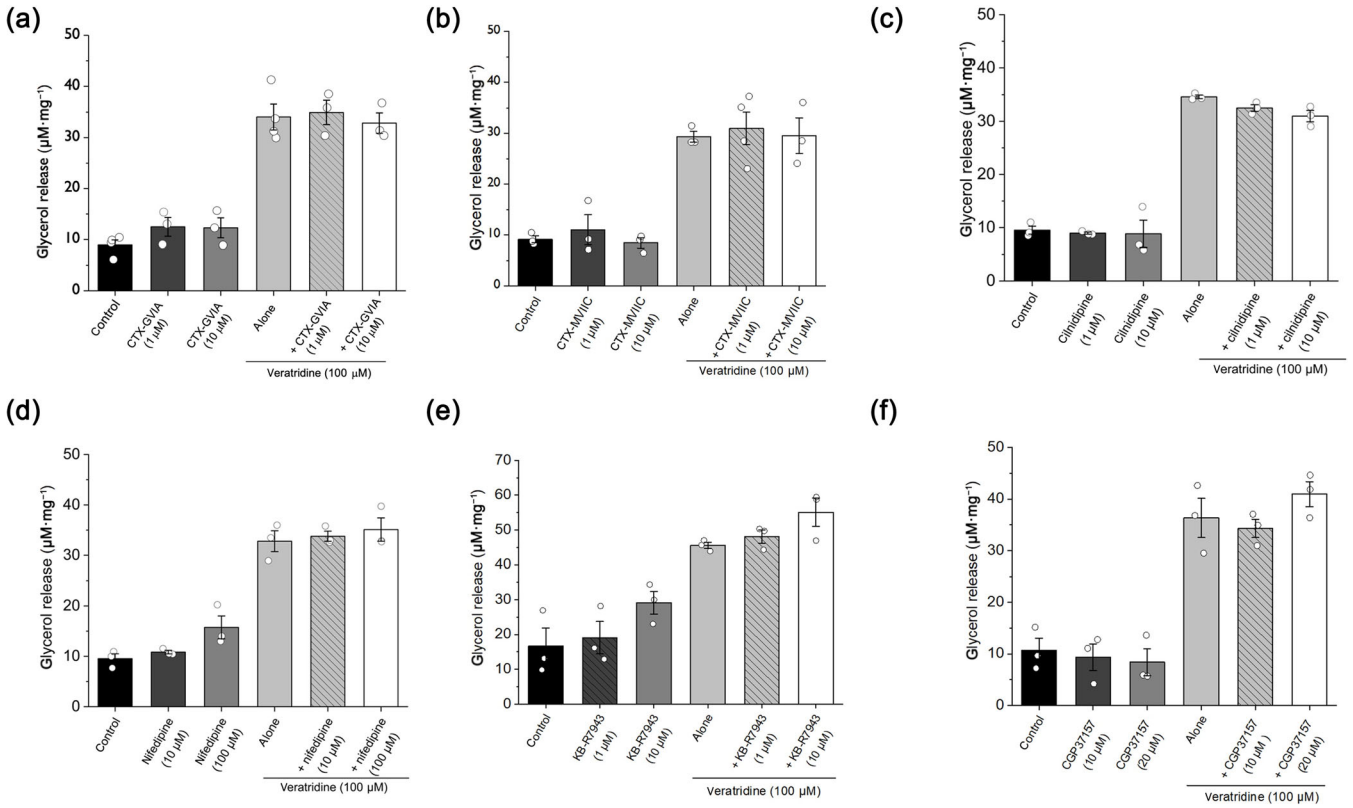

FIGURE 4 Veratridine-evoked glycerol release is insensitive to inhibition of voltage-gated Ca^{2+} channels or Na^+/Ca^{2+}-exchangers in white adipose tissue. (a) Peptide voltage-gated Ca^{2+} channel antagonists Ω-conotoxin GVIA (CTX-GVIA) or (b) Ω-conotoxin MVIIC (CTX-MVIIC) have no effect on basal glycerol release or veratridine-evoked glycerol release (N = 3–4). Small-molecule voltage-gated Ca^{2+} channel antagonists (c) cilnidipine and (d) nifedipine have no effect on basal glycerol release or veratridine-evoked glycerol release (3 h; N = 3). (e) Reverse-mode Na^+/Ca^{2+}-exchanger antagonist KB-R7943 or (f) mitochondrial Na^+/Ca^{2+}-exchanger antagonist GP37157 has no effect on basal glycerol release or veratridine-evoked glycerol release (N = 3). All responses are measured after 3 h. Glycerol released is expressed as $\mu M \cdot mg^{-1}$ wet tissue. Tissue was pre-incubated with antagonists for 30 min at room temperature prior to stimulation.

(Figure 4b). We also investigated the contribution of voltage-gated Ca^{2+} channels using small-molecule inhibitors, namely, **cilnidipine** (N-type and L-type) and **nifedipine** (L-type), and found that neither had any apparent effect on veratridine-evoked glycerol release or the basal rate of glycerol release (Figure 4c,d). The apparent lack of contribution of voltage-gated Ca^{2+} led us to investigate whether reverse **Na^+/Ca^{2+} or mitochondrial Na^+/Ca^{2+} exchangers** using the antagonists **KB-R7943** and **CGP37157**, respectively, as both exchangers have previously been implicated in neurotransmitter release. However, neither KB-R7943 nor CGP37157 had any apparent effect on veratridine-mediated glycerol release or basal glycerol release (Figure 4e,f), suggesting no involvement of Na^+/Ca^{2+} exchange.

We next investigated the dependency of veratridine-mediated glycerol release of sympathetic and sensory neurotransmitters. We investigated sensory neurotransmitters as our immunocytochemical studies revealed that tyrosine hydroxylase-positive and tyrosine hydroxylase-negative neurons innervate white adipose (Figure 1), and previous work has suggested that sensory neuropeptides can regulate lipolysis in white adipose. However, neither the selective natural killer (NK) receptor (for **substance P**) antagonist CP 96345 (Figure 5a) nor the selective CGRP receptor antagonist **BIBN 4096** (olcegepant) (Figure 5b) had any effect on veratridine-mediated glycerol release or basal glycerol release. We also probed the contribution of the sympathetic neurotransmitters **neuropeptide Y (NPY)**, **ATP** and noradrenaline. NPY receptors were investigated by selectively antagonising **Y_1**, **Y_2** or **Y_5** receptors with **BIBO3304**, **BIIE 0246** or **L-152804**, respectively. Neither BIBO3304 (Figure 5c), BIIE 0246 (Figure 5d) nor L-152804 (Figure 5e) had any effect on basal glycerol release or veratridine-mediated glycerol release, excluding a contribution of NPY in these experiments. We employed the broad-spectrum purinergic receptor antagonists **PPADS** and **suramin** to explore the contribution of ATP. Both PPADS (Figure 5f) and suramin (Figure 5g) had no effect on veratridine-mediated glycerol release or basal glycerol release.

Next, we investigated the involvement of β-adrenoceptors for noradrenaline in the veratridine-mediated glycerol release (Figure 6). The non-selective β-adrenoceptor antagonist **propranolol** abolished the response to veratridine, suggesting that β-adrenoceptor activity is essential for veratridine-mediated glycerol release in white adipose tissue (Figure 6a). Propranolol had no effect on basal glycerol release (Figure 6a). We employed selective antagonists of **β_1**-, **β_2**- and **β_3**-adrenoceptor subtypes, as all have previously been detected in white adipose tissue. The β_1-adrenoceptor selective antagonist **CGP**

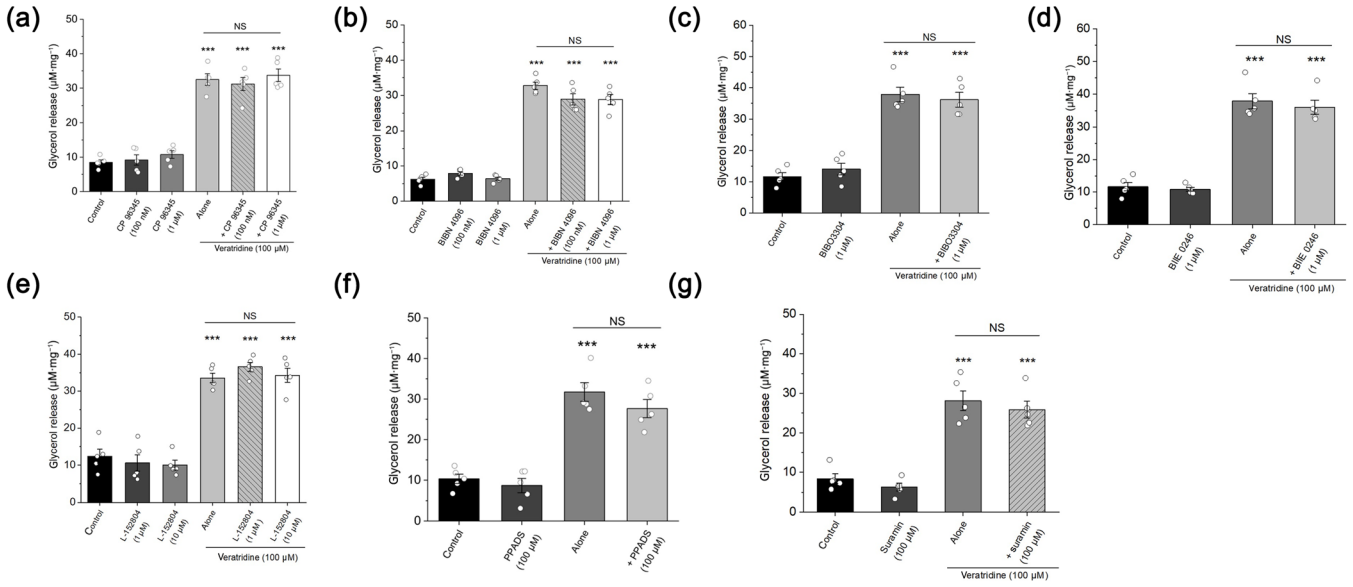

FIGURE 5 No contribution of sensory nerve peptides neurotransmitters or sympathetic nerve neurotransmitters neuropeptide Y or ATP to veratridine-evoked glycerol release in white adipose tissue. (a) NK_1 receptor selective antagonist CP 96345 or (b) calcitonin gene-related peptide 1 receptor selective antagonist BIBN 4096 BS has no effect on basal glycerol release or veratridine-evoked glycerol release (N = 5). Antagonism of neuropeptide Y signalling through (c) Y_1 receptors with BIBO3304, (d) Y_2 receptors with BIIE 0246 or (e) Y_5 receptors with L-152804 had no effect on basal glycerol release or veratridine-evoked glycerol release (N = 5). Inhibition of purinergic signalling with broad-spectrum antagonists (f) PPADS or (g) suramin had no effect on basal glycerol release or veratridine-evoked glycerol release (N = 5). $^{***}P < 0.001$, significantly different from vehicle control or between test and control groups for (c) and (f). $^{\#}P < 0.05$, $^{\#\#\#}P < 0.001$, significantly different as indicated; NS, no significance between compared groups. All responses are measured after 3 h. Glycerol released is expressed as $\mu M \cdot mg^{-1}$ wet tissue. Tissue was pre-incubated with antagonists for 30 min at room temperature prior to stimulation.

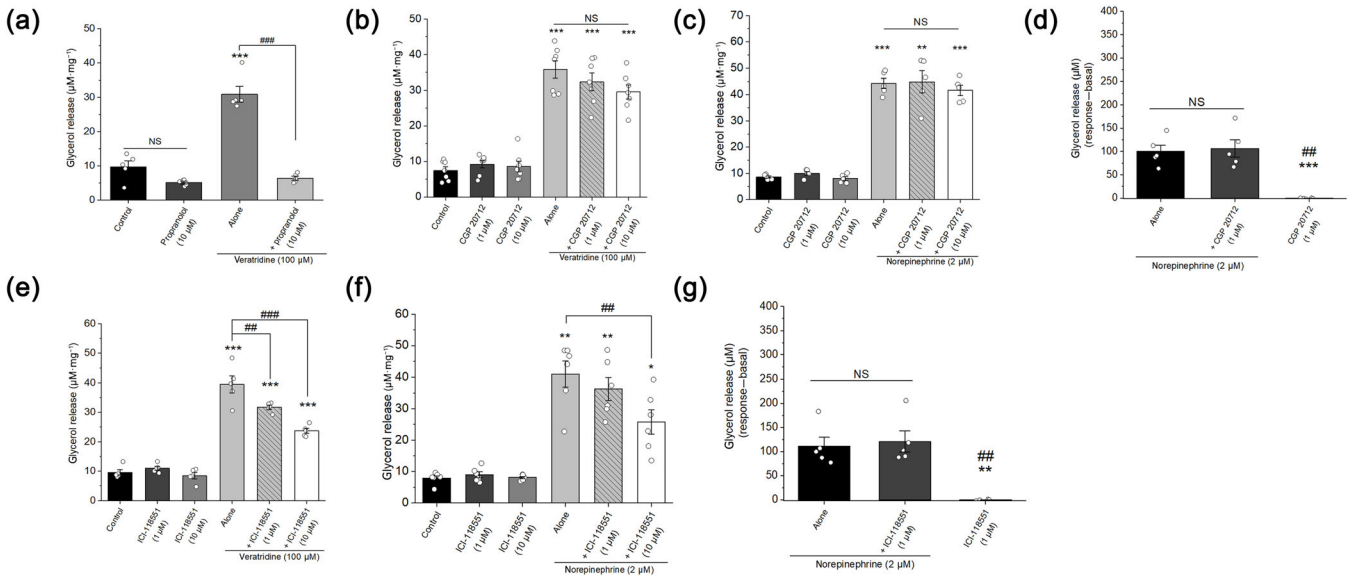

FIGURE 6 The β_2-adrenoceptors but not β_1-adrenoceptors contribute to veratridine-evoked glycerol release in white adipose tissue. (a) Abolition of veratridine-evoked glycerol release by non-selective β-adrenergic receptor antagonist propranolol (N = 5). No effect of β_1-adrenoceptor selective antagonist CGP 20712 on (b) veratridine-evoked (N = 7) or (c) noradrenaline-evoked glycerol release in white adipose tissue (N = 5). (d) CGP 20712 did not inhibit noradrenaline-evoked glycerol release in isolated white adipocytes (N = 5). Selective antagonism of β_2-adrenoceptors with ICI-118551 inhibits (e) veratridine-evoked glycerol release and (f) noradrenaline-evoked glycerol release in white adipose tissue (N = 5). (g) ICI-118551 did not inhibit noradrenaline-evoked glycerol release in isolated white adipocytes (N = 5). $^{*}P < 0.05$, $^{**}P < 0.01$, $^{***}P < 0.001$, significantly different from vehicle control. $^{\#\#}P < 0.01$, $^{\#\#\#}P < 0.001$, significantly different as indicated; NS, no significance between compared groups. All responses are measured after 3 h. Glycerol released is expressed as $\mu M \cdot mg^{-1}$ wet tissue. For adipocytes, glycerol release is expressed as μM, and basal glycerol release from untreated cells is subtracted from all test measurements. Tissue and cells were pre-incubated with antagonists for 30 min at room temperature prior to stimulation.

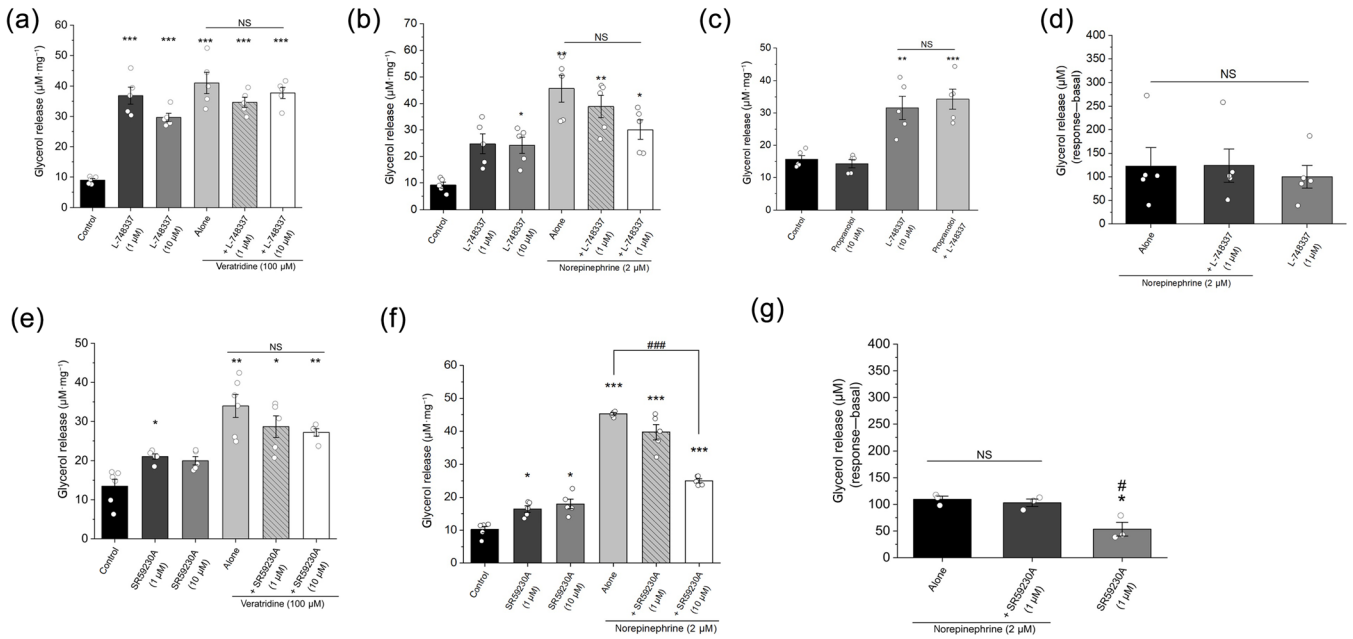

FIGURE 7 Selective β_3-adrenoceptor antagonists stimulate glycerol release in white adipose tissue and isolated white adipocytes. (a) Selective β_3-adrenoceptor antagonist L-748337 stimulates glycerol release in white adipose tissue but does not inhibit veratridine-evoked glycerol release (N = 5). (b) L-748337 does not inhibit noradrenaline-evoked glycerol release in white adipose tissue (N = 5). (c) L-748337-stimulated glycerol release is not antagonised by non-selective β-receptor antagonist propranolol (N = 5). (d) L-748337 stimulates glycerol release in isolated white adipocytes but does not inhibit norepinephrine-evoked glycerol release (N = 5). (e) Selective β_3-adrenoceptor antagonist SR59230A stimulates glycerol release in white adipose tissue but does not inhibit veratridine-evoked glycerol release (N = 5). (f) SR59230A inhibits noradrenaline-evoked glycerol release in white adipose tissue (N = 5). (g) SR59230A stimulates glycerol release in isolated adipocytes but does not inhibit noradrenaline-evoked release (N = 5). $^{*}P < 0.05$, $^{**}P < 0.01$, $^{***}P < 0.001$, significantly different from vehicle control. $^{\#\#\#}P < 0.001$, significantly different as indicated; NS, no significance between compared groups. All responses are measured after 3 h. Glycerol released is expressed as $\mu M \cdot mg^{-1}$ wet tissue. For adipocytes, glycerol release is expressed as μM, and basal glycerol release from untreated cells is subtracted from all test measurements. Tissue and cells were pre-incubated with antagonists for 30 min at room temperature prior to stimulation.

20712A did not inhibit the response to veratridine nor have any effect on basal glycerol release (Figure 6b). Glycerol release in response to noradrenaline was also insensitive to CGP 20712A (Figure 6c). CGP 20712A did not inhibit noradrenaline -evoked glycerol release in isolated adipocytes (Figure 6d). The β_2-adrenoceptor selective antagonist **ICI-118551** significantly inhibited both glycerol release in response to veratridine (Figure 6e) and to noradrenaline (Figure 6f), but was without effect on basal glycerol release. ICI-118551 did not inhibit noradrenaline -evoked glycerol release in isolated adipocytes (Figure 6g).

The β_3-adrenoceptor selective antagonist **L748337** had an unexpected effect on glycerol release in white adipose tissue. L748337 alone stimulated glycerol release to a level comparable to that of veratridine (Figure 7a) and a half-maximal concentration of noradrenaline (Figure 7b). The stimulating effects of L748337 in combination with veratridine or noradrenaline had no greater effect than veratridine or noradrenaline alone (Figure 7a,b). L748337 did not antagonise glycerol release stimulated by veratridine or noradrenaline (Figure 7a,b). The lipolytic effect of L748337 was not antagonised by propranolol (Figure 7c). To investigate whether the stimulatory effect of L748337 was directly upon adipocytes or dependent upon another cell type present in white adipose tissue, we conducted further experiments in freshly isolated adipocytes. In these experiments, L748337 again stimulated glycerol release to a level comparable to a half-maximal concentration of noradrenaline (Figure 7d). L748337 did not antagonise glycerol release stimulated by noradrenaline in isolated adipocytes (Figure 7d). Another β_3-adrenoceptor antagonist **SR59230A** was also tested. In these experiments, SR59230A also has lipolytic effects in adipose tissue (Figure 7e) but could not antagonise veratridine-mediated glycerol release (Figure 7e). SR59230A at 10 μM did partly inhibit noradrenaline-mediated glycerol release in adipose tissue (Figure 7f). SR59230A also had a direct lipolytic effect in isolated adipocytes (Figure 7g). These data suggest that two chemically distinct β_3-adrenoceptor antagonists stimulated lipolysis in mouse white adipose tissue and freshly isolated white adipocytes. Finally, to link the glycerol release with β-adrenoceptor activity and the mechanism of action of veratridine, we sought direct evidence that veratridine can stimulate noradrenaline release in white adipose tissue. In experiments to measure adipose tissue outflow of noradrenaline upon veratridine stimulation, we observed time-dependent release of noradrenaline into the medium (Figure 8a). Noradrenaline release was not observed in unchallenged control tissue (Figure 8b). Importantly, and as observed for glycerol release, TTX abolished the ability of veratridine to stimulate noradrenaline release (Figure 8b). Taken

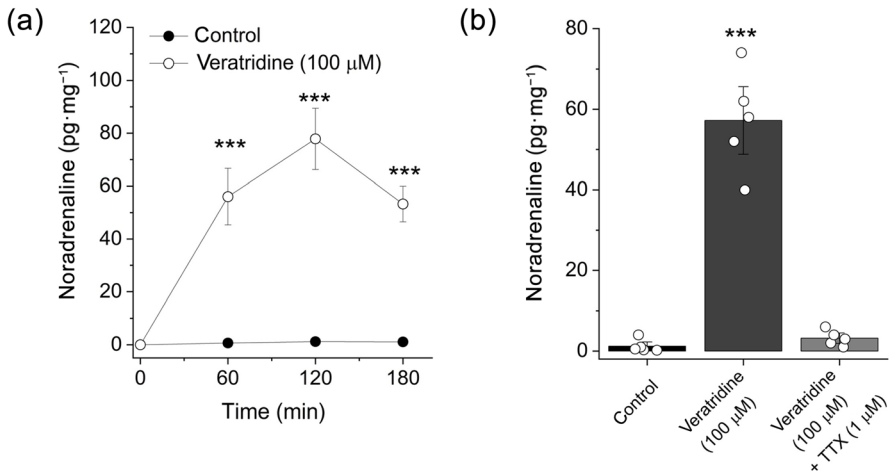

FIGURE 8 Veratridine stimulates noradrenaline outflow in white adipose tissue. (a) Veratridine stimulates time-dependent release of noradrenaline from white adipose tissue, compared to tissue treated with vehicle control (*control*) (N = 5). (b) Release of noradrenaline measured 3 h after veratridine treatment is abolished by tetrodotoxin (TTX) (N = 5). Control is treated with the vehicle alone. In all experiments, the amount of noradrenaline detectable in medium is normalised to the mass of adipose tissue. $^{***}P < 0.001$, significantly different from vehicle control. Tissue was pre-incubated with antagonists for 30 min at room temperature prior to stimulation.

together, these data support a mechanism of action whereby veratridine stimulates sympathetic nerve activity in white adipose tissue, causing the release of noradrenaline, which subsequently stimulates lipolysis through activation of β_2-adrenoceptors.

4 | DISCUSSION

Our immunocytochemistry data support innervation of white adipose tissue including that of the medium and large blood vessels that perfuse it and of the adipocytes themselves. Veratridine is a plant-derived alkaloid widely used as an opener of voltage-gated sodium channels, sustaining channel opening by inhibiting channel inactivation (Zhang et al., 2018). Veratridine therefore increases nervous activity by promoting membrane depolarisation and action potential firing. Veratridine is known to stimulate catecholamine secretion from adrenal chromaffin cells (Nemoto et al., 2013) and elicits bursting activity (Otoom & Alkadhi, 2000) and calcium responses in neurons (Mohammed et al., 2017). We observed that the effect of veratridine was completely reversed by TTX, suggesting that activation of TTX-sensitive, voltage-gated, Na^+ channels underpins the observed glycerol release in white adipose tissue. The cellular target of veratridine in white adipose tissue is highly likely to be neurons, as its effects on glycerol release were absent in isolated adipocytes and abolished by propranolol. TTX-sensitive voltage-gated Na^+ channels are well documented in sensory neurons (Pinto et al., 2008) but are also functional in sympathetic neurons (Kim et al., 2024; Minett et al., 2012). Our data exclude involvement of sensory neuropeptides in the response to veratridine and therefore no obvious role of sensory neurons, although they were present in the adipose tissue. We propose therefore that the action of veratridine is to evoke release of neurotransmitters from sympathetic nerves that act upon adipocytes to stimulate lipolysis. Action potential stimulation of neurotransmitter release in neurons is associated with external Ca^{2+}-dependent and independent mechanisms (Adam-Vizi, 1992). Our study reveals that adipose tissue ex vivo releases glycerol when unstimulated, suggesting a basal rate of lipolysis. This is consistent with our previous studies of human adipocytes (Ali et al., 2018a), which also exhibit basal lipolysis. Basal lipolysis is increased in hypertrophic adipocytes, in models of diet-induced obesity (Wueest et al., 2009). Our data reveal that basal lipolysis was insensitive to TTX, which suggests that neuronal activity did not mediate basal lipolysis. This would be consistent with our finding that isolated adipocytes exhibited basal lipolysis (Ali et al., 2018a). The lack of effect of propranolol and sensory neuropeptide receptor antagonists on basal lipolysis also supports no role of nervous activity. The pharmacology of veratridine-evoked glycerol release suggests no involvement of voltage-gated Ca^{2+} channels or Ca^{2+}/Na^+-exchange mechanisms, as described in previous studies of regulated neurotransmitter release (Parnis et al., 2013; Parpura et al., 2011). Our suggestion that the action of veratridine is independent of Ca^{2+} is supported by a number of studies using brain slices, where veratridine stimulates neurotransmitter release, independent of Ca^{2+} but blocked by TTX (Cunningham & Neal, 1981; Liang & Rutledge, 1983). However, some studies do suggest a contribution of voltage-gated Ca^{2+} channels to veratridine-evoked neurotransmitter release (Dobrev et al., 1998). Further studies have suggested that veratridine-evoked Na^+ influx and depolarisation trigger neurotransmitter release without requirement for extracellular Ca^{2+} (Levi et al., 1980). A feasible explanation for the Ca^{2+}-independent effect of veratridine is via neuronal swelling demonstrated previously in brain slice preparations using veratridine (Rungta et al., 2015), as Na^+ influx-induced swelling can trigger exocytosis in a Ca^{2+}-independent fashion (Fedorovich et al., 2005).

Though ATP and NPY are released by sympathetic nerves as co-transmitters with noradrenaline (Gonzalez-Montelongo et al., 2023; Gonzalez-Montelongo & Fountain, 2021), we exclude a contribution of both to stimulated or basal lipolysis in this preparation. We have previously described a role for purinergic signalling in controlling lipolysis in human adipocytes and intracellular Ca^{2+} responses in human adipose-derived mesenchymal stromal cells (Ali et al., 2018a, 2018b). NPY knockout mice have reduced adiposity (Park et al., 2014), though whether this occurs due to loss of central or peripheral NPY activity is not clear. Studies in mouse epididymal white adipocytes have shown that NPY addition suppresses basal lipolysis and stimulates lipolysis in

response to some receptor ligands (Bradley et al., 2005). Our study does, however, fully support a contribution of β-adrenoceptor signalling in veratridine- and noradrenaline-evoked glycerol release. The response to veratridine was abolished by propranolol, in concentrations shown to fully antagonise mouse β_1-, β_2- and β_3-adrenoceptors (Nahmias et al., 1991; Popp et al., 2004). The selective β_1-adrenoceptor antagonist CGP 20712A (Dooley et al., 1986) did not block veratridine- or noradrenaline-evoked glycerol release. Our study is in disagreement with the study of Louis et al. (2000) who investigated the contribution of β-adrenoceptor subtype to lipolysis in rat isolated epididymal white adipocytes. In another study (Collins et al., 1994), the authors suggested that the contribution of β_1-adrenoceptors to lipolysis may be dependent upon the concentration of noradrenaline. In our experiments, we used an approximate EC_{50} value of noradrenaline and it is possible that β_1-adrenoceptors do contribute to noradrenaline-evoked lipolysis in tissue and adipocytes at lower concentrations of noradrenaline. The β_1-adrenoceptor antagonist CGP 20712 blocked isoprenaline-induced glycerol release in primary epididymal fat adipocytes from high-fat diet-fed mice (Li et al., 2015). Our finding that β_2-adrenoceptors were involved in stimulated lipolysis in mouse adipose tissue is novel but consistent with observations in human adipocytes (Hoffstedt et al., 1995). Interestingly, we found that β_2-adrenoceptors did contribute to noradrenaline-evoked glycerol release in adipose tissue, but not in isolated adipocytes. In our study, 10-μM ICI-118551 was required to observe inhibition in adipose tissue, though we only tested up to 1-μM ICI-118551 in an effort to mimic the effect observed on veratridine-evoked glycerol release in tissue. The difference in sensitivity of glycerol release responses to ICI-118551 could be reflective of a graded contribution of β-adrenoceptor subtypes to noradrenaline concentrations in tissue (Louis et al., 2000). Via either veratridine-stimulated release or exogenous noradrenaline application, noradrenaline exposure of adipocytes in whole tissue is likely differ significantly from that in preparations of isolated cells, due to active noradrenaline-scavenging mechanisms known to be present in adipose tissue (Ryuid & Buettner, 2019), which includes vascular cell types (Horvath et al., 2003).

L748337 and SR59230A were both developed as selective β_3-adrenoceptor antagonists, though their β_3-selectivity has been questioned (Hoffmann et al., 2004; Schena & Caplan, 2019). In rodents, β_3-adrenoceptors have been ascribed roles in thermogenesis in brown adipocytes and lipolysis in white adipocytes, though the role of β_3-adrenoceptors in human adipocytes appears less important. Our experiments revealed that both L748337 and SR59230A stimulated lipolysis in mouse inguinal white adipose tissue and in adipocytes isolated from this tissue. This observation is intriguing but perhaps not unexpected, as several studies indicate that the L748337 and SR59230A have partial agonist activity (Sato et al., 2007, 2008). In CHO-K1 expressing the human or mouse β_3-adrenoceptor, both ligands stimulated phosphorylation of **p38 MAP kinase** (Sato et al., 2007, 2008), a response reversed by *Pertussis* toxin suggesting involvement of G_i G-protein-dependent signalling. Promiscuous coupling of β_3-adrenoceptors to G_i-dependent pathways in adipocytes has been demonstrated (Robidoux et al., 2006; Soeder et al., 1999), and p38 MAP kinase signalling drives lipolysis (El-Merahbi et al., 2020). However, in this study, the effect of both L748337 and SR59230A on basal lipolysis made it difficult to determine whether β_3-adrenoceptors were involved in veratridine-mediated glycerol release or not. SR59230A could antagonise the lipolytic response to noradrenaline in adipose tissue, suggesting that β_3-adrenoceptor activation could stimulate lipolysis in murine inguinal white adipose tissue.

The pharmacological differences observed in our study compared to others may be due to a number of factors including differences in the pharmacology of anatomically distinct white adipose tissue sites in rodents (Chusyd et al., 2016) or the involvement of distinct receptor subtypes at different levels of nervous activity. A more refined experimental control of nervous activity in white adipose tissue may allow for a more graded approach and assessment of the contribution of adipocyte receptors at different levels of nervous activity, potentially through optogenetics or a direct electrical stimulation approach. An experimental ability to grade sympathetic nerve activity will be important when modelling sympathetic hyperactivity associated with metabolic syndrome.

The amounts of tissue required for the assays described in this study are relatively small, with multiple samples available from a single mouse when white inguinal adipose is studied. This provides an opportunity to limit animal usage for ex vivo studies compared to studies using isolated adipocytes, which in general require larger amounts of tissue and potential pooling of tissue from several animals. The findings of this study are not clinically relevant regarding the use of veratridine to drive lipolysis, as veratridine is likely to produce adverse neurotoxic effects in vivo. However, the model provides an opportunity to validate novel pharmacological agents designed to manipulate the control of white adipose tissue by the nervous system.

In summary, our study showed that pharmacological activation of sympathetic nerves in white adipose tissue with veratridine can be used to study neurogenic lipolysis in adipose tissue ex vivo. We reveal the mechanism of veratridine action is sensitive to TTX but insensitive to antagonists of voltage-gated Ca^{2+} channels and Na^+/Ca^{2+} exchangers. The lipolytic response of white adipose tissue to sympathetic nerve activation was solely through β-adrenoceptors, specifically via activation of β_2-adrenoceptors.

AUTHOR CONTRIBUTIONS

Kayleigh E. Goddard: Data curation; formal analysis; investigation; methodology; validation; visualization; writing—review and editing. **Samuel J. Fountain:** Conceptualization; data curation; formal analysis; funding acquisition; investigation; methodology; project administration; supervision; visualization; writing—original draft; writing—review and editing.

ACKNOWLEDGEMENTS

This work was funded by the Biotechnology and Biological Sciences Research Council and the British Heart Foundation (PG/19/35/34389).

CONFLICT OF INTEREST STATEMENT

None.

DATA AVAILABILITY STATEMENT

The data that support the findings of this study are available from the corresponding author upon reasonable request.

DECLARATION OF TRANSPARENCY AND SCIENTIFIC RIGOUR

This Declaration acknowledges that this paper adheres to the principles for transparent reporting and scientific rigour of preclinical research as stated in the *BJP* guidelines for Design & Analysis, Immunoblotting and Immunochemistry, and Animal Experimentation and as recommended by funding agencies, publishers and other organisations engaged with supporting research.

ORCID

Samuel J. Fountain https://orcid.org/0000-0002-6028-0548

REFERENCES

Adam-Vizi, V. (1992). External Ca^{2+}-independent release of neurotransmitters. *Journal of Neurochemistry*, *58*(2), 395–405. https://doi.org/10.1111/j.1471-4159.1992.tb09736.x

Alexander, S. P. H., Christopoulos, A., Davenport, A. P., Kelly, E., Mathie, A. A., Peters, J. A., Veale, E. L., Armstrong, J. F., Faccenda, E., Harding, S. D., Davies, J. A., Abbracchio, M. P., Abraham, G., Agoulnik, A., Alexander, W., Al-Hosaini, K., Bäck, M., Baker, J. G., Barnes, N. M., … Ye, R. D. (2023). The Concise Guide to PHARMACOLOGY 2023/24: G protein-coupled receptors. *British Journal of Pharmacology*, *180*(Suppl 2), S23–S144. https://doi.org/10.1111/bph.16177

Alexander, S. P. H., Fabbro, D., Kelly, E., Mathie, A. A., Peters, J. A., Veale, E. L., Armstrong, J. F., Faccenda, E., Harding, S. D., Davies, J. A., Amarosi, L., Anderson, C. M. H., Beart, P. M., Broer, S., Dawson, P. A., Gyimesi, G., Hagenbuch, B., Hammond, J. R., Hancox, J. C., … Verri, T. (2023). The Concise Guide to PHARMACOLOGY 2023/24: Transporters. *British Journal of Pharmacology*, *180*(Suppl 2), S374–S469. https://doi.org/10.1111/bph.16182

Alexander, S. P. H., Fabbro, D., Kelly, E., Mathie, A. A., Peters, J. A., Veale, E. L., Armstrong, J. F., Faccenda, E., Harding, S. D., Davies, J. A., Annett, S., Boison, D., Burns, K. E., Dessauer, C., Gertsch, J., Helsby, N. A., Izzo, A. A., Ostrom, R., Papapetropoulos, A., … Wong, S. S. (2023). The Concise Guide to PHARMACOLOGY 2023/24: Enzymes. *British Journal of Pharmacology*, *180*(Suppl 2), S289–S373. https://doi.org/10.1111/bph.16181

Alexander, S. P. H., Fabbro, D., Kelly, E., Mathie, A. A., Peters, J. A., Veale, E. L., Armstrong, J. F., Faccenda, E., Harding, S. D., Davies, J. A., Beuve, A., Brouckaert, P., Bryant, C., Burnett, J. C., Farndale, R. W., Friebe, A., Garthwaite, J., Hobbs, A. J., Jarvis, G. E., … Waldman, S. A. (2023). The Concise Guide to PHARMACOLOGY 2023/24: Catalytic receptors. *British Journal of Pharmacology*, *180*(Suppl 2), S241–S288. https://doi.org/10.1111/bph.16180

Alexander, S. P. H., Kelly, E., Mathie, A. A., Peters, J. A., Veale, E. L., Armstrong, J. F., Buneman, O. P., Faccenda, E., Harding, S. D., Spedding, M., Cidlowski, J. A., Fabbro, D., Davenport, A. P., Striessnig, J., Davies, J. A., Ahlers-Dannen, K. E., Alqinyah, M., Arumugam, T. V., Bodle, C., … Zolghadri, Y. (2023). The Concise Guide to PHARMACOLOGY 2023/24: Introduction and Other Protein Targets. *British Journal of Pharmacology*, *180*, S1–S22. https://doi.org/10.1111/bph.16176

Alexander, S. P. H., Mathie, A. A., Peters, J. A., Veale, E. L., Striessnig, J., Kelly, E., Armstrong, J. F., Faccenda, E., Harding, S. D., Davies, J. A., Aldrich, R. W., Attali, B., Baggetta, A. M., Becirovic, E., Biel, M., Bill, R. M., Caceres, A. I., Catterall, W. A., Conner, A. C., … Zhu, M. (2023). The Concise Guide to PHARMACOLOGY 2023/24: Ion channels. *British Journal of Pharmacology*, *180*(Suppl 2), S145–S222. https://doi.org/10.1111/bph.16181

Ali, S., Turner, J., & Fountain, S. J. (2018b). $P2Y_2$ and $P2Y_6$ receptor activation elicits intracellular calcium responses in human adipose-derived mesenchymal stromal cells. *Purinergic Signalling*, *14*(4), 371–384. https://doi.org/10.1007/s11302-018-9618-3

Ali, S. B., Turner, J. J. O., & Fountain, S. J. (2018a). Constitutive $P2Y_2$ receptor activity regulates basal lipolysis in human adipocytes. *Journal of Cell Science*, *131*(22). https://doi.org/10.1242/jcs.221994

Bartness, T. J., Liu, Y., Shrestha, Y. B., & Ryu, V. (2014). Neural innervation of white adipose tissue and the control of lipolysis. *Frontiers in Neuroendocrinology*, *35*(4), 473–493. https://doi.org/10.1016/j.yfrne.2014.04.001

Bowers, R. R., Festuccia, W. T., Song, C. K., Shi, H., Migliorini, R. H., & Bartness, T. J. (2004). Sympathetic innervation of white adipose tissue and its regulation of fat cell number. *American Journal of Physiology. Regulatory, Integrative and Comparative Physiology*, *286*, 1167–1175. https://doi.org/10.1152/ajpregu.00558.2003.-White

Bradley, R. L., Mansfield, J. P. R., & Maratos-Flier, E. (2005). Neuropeptides, including neuropeptide Y and melanocortins, mediate lipolysis in murine adipocytes. *Obesity Research*, *13*(4), 653–661. https://doi.org/10.1038/oby.2005.73

Casimiro, I., Stull, N. D., Tersey, S. A., & Mirmira, R. G. (2021). Phenotypic sexual dimorphism in response to dietary fat manipulation in C57BL/6J mice. *Journal of Diabetes and its Complications*, *35*(2), 107795. https://doi.org/10.1016/j.jdiacomp.2020.107795

Chusyd, D. E., Wang, D., Huffman, D. M., & Nagy, T. R. (2016). Relationships between rodent white adipose fat pads and human white adipose fat depots. *Frontiers in Nutrition*, *3*. https://doi.org/10.3389/fnut.2016.00010

Collins, S., Daniel, K. W., Rohlfs, E. M., Ramkumart, V., Taylor, I. L., & Gettys, T. W. (1994). Impaired expression and functional activity of the beta 3- and beta 1-adrenergic receptors in adipose tissue of congenitally obese (C57BL/6J ob/ob) mice. *Molecular Endocrinology*, *8*(4), 518–527. https://doi.org/10.1210/mend.8.4.7914350

Cunningham, J. O., & Neal, M. J. (1981). On the mechanism by which veratridine causes a calcium-independent release of γ-aminobutyric acid from brain slices. *British Journal of Pharmacology*, *73*, 655–667. https://doi.org/10.1111/j.1476-5381.1981.tb16801.x

Curtis, M. J., Alexander, S. P. H., Cirino, G., George, C. H., Kendall, D. A., Insel, P. A., Izzo, A. A., Ji, Y., Panettieri, R. A., Patel, H. H., Sobey, C. G., Stanford, S. C., Stanley, P., Stefanska, B., Stephens, G. J., Teixeira, M. M., Vergnolle, N., & Ahluwalia, A. (2022). Planning experiments: Updated guidance on experimental design and analysis and their reporting III. *British Journal of Pharmacology*, *179*, 3907–3913. https://doi.org/10.1111/bph.15868

Dobrev, D., Milde, A. S., Andreas, K., & Ravens, U. (1998). Voltage-activated calcium channels involved in veratridine-evoked [^{3}H]dopamine release in rat striatal slices. *Neuropharmacology*, *37*, 973–982. https://doi.org/10.1016/S0028-3908(98)00103-8

Doevendans, P. A., Daemen, M. J., De Muinck, E. D., & Smits, J. F. (1998). Cardiovascular phenotyping in mice. *Cardiovascular Research*, *39*, 34–49. https://doi.org/10.1016/S0008-6363(98)00073-X

Dooley, D. J., Bittiger, H., & Reymann, N. C. (1986). CGP 20712 A: A useful tool for quantitating β_1- and β_2-adrenoceptors. *European Journal of Pharmacology*, *130*, 137–139. https://doi.org/10.1016/0014-2999(86)90193-7

El-Merahbi, R., Viera, J. T., Valdes, A. L., Kolczynska, K., Reuter, S., Löffler, M. C., Erk, M., Ade, C. P., Karwen, T., Mayer, A. E., Eilers, M., & Sumara, G. (2020). The adrenergic-induced ERK3 pathway drives

lipolysis and suppresses energy dissipation. *Genes and Development*, *34*(7–8), 495–510. https://doi.org/10.1101/gad.333617.119

Esler, M., Lambert, G., Schlaich, M., Dixon, J., Sari, C. I., & Lambert, E. (2018). Obesity paradox in hypertension: Is this because sympathetic activation in obesity-hypertension takes a benign form? *Hypertension*, *71*(1), 22–33. https://doi.org/10.1161/HYPERTENSIONAHA.117.09790

Fedorenko, O. A., Pulbutr, P., Banke, E., Akaniro-Ejim, N. E., Bentley, D. C., Olofsson, C. S., Chan, S., & Smith, P. A. (2020). CaV1.2 and CaV1.3 voltage-gated L-type Ca^{2+} channels in rat white fat adipocytes. *Journal of Endocrinology*, *244*(2), 369–381. https://doi.org/10.1530/JOE-19-0493

Fedorovich, S. V., Waseem, T. V., Lavrukevich, T. V., & Konev, S. V. (2005). Role of calcium in exocytosis induced by hypotonic swelling. *Annals of the New York Academy of Sciences*, *1048*, 337–340. https://doi.org/10.1196/annals.1342.031

Gonzalez-Montelongo, M. C., & Fountain, S. J. (2021). Neuropeptide Y facilitates P2X1 receptor-dependent vasoconstriction via Y1 receptor activation in small mesenteric arteries during sympathetic neurogenic responses. *Vascular Pharmacology*, *136*, 106810. https://doi.org/10.1016/j.vph.2020.106810

Gonzalez-Montelongo, M. D. C., Meades, J. L., Fortuny-Gomez, A., & Fountain, S. J. (2023). Neuropeptide Y: Direct vasoconstrictor and facilitatory effects on P2X1 receptor-dependent vasoconstriction in human small abdominal arteries. *Vascular Pharmacology*, *151*, 107192. https://doi.org/10.1016/j.vph.2023.107192

Hoffmann, C., Leitz, M. R., Oberdorf-Maass, S., Lohse, M. J., & Klotz, K. N. (2004). Comparative pharmacology of human β-adrenergic receptor subtypes—Characterization of stably transfected receptors in CHO cells. *Naunyn-Schmiedeberg's Archives of Pharmacology*, *369*(2), 151–159. https://doi.org/10.1007/s00210-003-0860-y

Hoffstedt, J., Shimizu, M., Sjöstedt, S., & Lönnqvist, F. (1995). Determination of β_3-adrenoceptor mediated lipolysis in human fat cells. *Obesity Research*, *3*(5), 447–457. https://doi.org/10.1002/j.1550-8528.1995.tb00174.x

Horvath, G., Sutto, Z., Torbati, A., Conner, G. E., Salathe, M., & Wanner, A. (2003). Norepinephrine transport by the extraneuronal monoamine transporter in human bronchial arterial smooth muscle cells. *American Journal of Physiology—Lung Cellular and Molecular Physiology*, *285*(4), L829–L837. https://doi.org/10.1152/ajplung.00054.2003

Kawai, T., Autieri, M. V., & Scalia, R. (2021). Adipose tissue inflammation and metabolic dysfunction in obesity. *American Journal of Physiology—Cell Physiology*, *320*(3), C375–C391. https://doi.org/10.1152/ajpcell.00379.2020

Kim, J. S., Meeker, S., Ru, F., Tran, M., Zabka, T. S., Hackos, D., & Undem, B. J. (2024). Role of $Na_V1.7$ in postganglionic sympathetic nerve function in human and guinea-pig arteries. *The Journal of Physiology*, *602*, 1–14. https://doi.org/10.1113/JP286538#support-information-section

Koenen, M., Hill, M. A., Cohen, P., & Sowers, J. R. (2021). Obesity, adipose tissue and vascular dysfunction. *Circulation Research*, *128*(7), 951–968. https://doi.org/10.1161/CIRCRESAHA.121.318093

Kusminski, C. M., Bickel, P. E., & Scherer, P. E. (2016). Targeting adipose tissue in the treatment of obesity-associated diabetes. *Nature Reviews in Drug Discovery*, *15*(9), 639–660. https://doi.org/10.1038/nrd.2016.75

Levi, G., Gallo, V., & Raiteri, M. (1980). A reevaluation of veratridine as a tool for studying the depolarization-induced release of neurotransmitters from nerve endings. *Neurochemical Research*, *5*(3), 281–295.

Li, J. J., Ferry, R. J. Jr., Diao, S., Xue, B., Bahouth, S. W., & Liao, F. F. (2015). Nedd4 haploinsufficient mice display moderate insulin resistance, enhanced lipolysis, and protection against high-fat diet-induced obesity. *Endocrinology (United States)*, *156*(4), 1283–1291. https://doi.org/10.1210/en.2014-1909

Liang, N. Y., & Rutledge, C. O. (1983). Calcium-independent release of [^{3}H] dopamine by veratridine in pargyline- and reserpine-treated corpus striatum. *European Journal of Pharmacology*, *89*, 153–155. https://doi.org/10.1016/0014-2999(83)90621-0

Lilley, E., Stanford, S. C., Kendall, D. E., Alexander, S. P. H., Cirino, G., Docherty, J. R., George, C. H., Insel, P. A., Izzo, A. A., Ji, Y., Panettieri, R. A., Sobey, C. G., Stefanska, B., Stephens, G., Teixeira, M., & Ahluwalia, A. (2020). ARRIVE 2.0 and the British Journal of Pharmacology: Updated guidance for 2020. *British Journal of Pharmacology*, *177*, 3611–3616. https://doi.org/10.1111/bph.15178

Louis, S. N. S., Jackman, G. P., Nero, T. L., Iakovidis, D., & Louis, W. J. (2000). Role of β-adrenergic receptor subtypes in lipolysis. *Cardiovascular Drugs and Therapy*, *14*, 565–577. https://doi.org/10.1023/A:1007838125152

Minett, M. S., Nassar, M. A., Clark, A. K., Passmore, G., Dickenson, A. H., Wang, F., Malcangio, M., & Wood, J. N. (2012). Distinct Nav1.7-dependent pain sensations require different sets of sensory and sympathetic neurons. *Nature Communications*, *3*, 791. https://doi.org/10.1038/ncomms1795

Mohammed, Z. A., Doran, C., Grundy, D., & Nassar, M. A. (2017). Veratridine produces distinct calcium response profiles in mouse dorsal root ganglia neurons. *Scientific Reports*, *7*, 45221. https://doi.org/10.1038/srep45221

Mowers, J., Uhm, M., Reilly, S. M., Simon, J., Leto, D., Chiang, S. H., Chang, L., & Saltiel, A. R. (2013). Inflammation produces catecholamine resistance in obesity via activation of PDE3B by the protein kinases IKKε and TBK1. *eLife*, *2013*(2), e01119. https://doi.org/10.7554/eLife.01119

Nahmias, C., Blin, N., Elalouf, J. M., Mattei, M. G., Strosberg, A. D., & Emorine, L. J. (1991). Molecular characterization of the mouse beta 3-adrenergic receptor: Relationship with the atypical receptor of adipocytes. *The EMBO Journal*, *10*(12), 3721–3727. https://doi.org/10.1002/j.1460-2075.1991.tb04940.x

Nemoto, T., Yanagita, T., Maruta, T., Sugita, C., Satoh, S., Kanai, T., Wada, A., & Murakami, M. (2013). Endothelin-1-induced down-regulation of $Na_V1.7$ expression in adrenal chromaffin cells: Attenuation of catecholamine secretion and tau dephosphorylation. *FEBS Letters*, *587*(7), 898–905. https://doi.org/10.1016/j.febslet.2013.02.013

Otoom, S. A., & Alkadhi, K. A. (2000). Epileptiform activity of veratridine model in rat brain slices: Effects of antiepileptic drugs. *Epilepsy Research*, *38*, 161–170. https://doi.org/10.1016/S0920-1211(99)00084-4

Park, S., Fujishita, C., Komatsu, T., Kim, S. E., Chiba, T., Mori, R., & Shimokawa, I. (2014). NPY antagonism reduces adiposity and attenuates age-related imbalance of adipose tissue metabolism. *FASEB Journal*, *28*(12), 5337–5348. https://doi.org/10.1096/fj.14-258384

Parnis, J., Montana, V., Delgado-Martinez, I., Matyash, V., Parpura, V., Kettenmann, H., Sekler, I., & Nolte, C. (2013). Mitochondrial exchanger NCLX plays a major role in the intracellular Ca^{2+} signaling, gliotransmission, and proliferation of astrocytes. *Journal of Neuroscience*, *33*(17), 7206–7219. https://doi.org/10.1523/JNEUROSCI.5721-12.2013

Parpura, V., Grubišic, V., & Verkhratsky, A. (2011). Ca^{2+} sources for the exocytotic release of glutamate from astrocytes. *Biochimica et Biophysica Acta—Molecular Cell Research*, *1813*(5), 984–991. https://doi.org/10.1016/j.bbamcr.2010.11.006

Percie du Sert, N., Hurst, V., Ahluwalia, A., Alam, S., Avey, M. T., Baker, M., Browne, W. J., Clark, A., Cuthill, I. C., Dirnagl, U., Emerson, M., Garner, P., Holgate, S. T., Howells, D. W., Karp, N. A., Lazic, S. E., Lidster, K., MacCallum, C. J., Macleod, M., … Würbel, H. (2020). The ARRIVE guidelines 2.0: Updated guidelines for reporting animal research. *PLoS Biology*, *18*(7), e3000410. https://doi.org/10.1371/journal.pbio.3000410

Pinto, V., Derkach, V. A., & Safronov, B. V. (2008). Role of TTX-sensitive and TTX-resistant sodium channels in Aδ- and C-fiber conduction and

synaptic transmission. *Journal of Neurophysiology*, *99*(2), 617–628. https://doi.org/10.1152/jn.00944.2007

Popp, B. D., Hutchinson, D. S., Evans, B. A., & Summers, R. J. (2004). Stereoselectivity for interactions of agonists and antagonists at mouse, rat and human β_3-adrenoceptors. *European Journal of Pharmacology*, *484*(2–3), 323–331. https://doi.org/10.1016/j.ejphar.2003.11.034

Robidoux, J., Kumar, N., Daniel, K. W., Moukdar, F., Cyr, M., Medvedev, A. V., & Collins, S. (2006). Maximal β_3-adrenergic regulation of lipolysis involves Src and epidermal growth factor receptor-dependent ERK1/2 activation. *Journal of Biological Chemistry*, *281*(49), 37794–37802. https://doi.org/10.1074/jbc.M605572200

Rungta, R. L., Choi, H. B., Tyson, J. R., Malik, A., Dissing-Olesen, L., Lin, P. J. C., Cain, S. M., Cullis, P. R., Snutch, T. P., & Macvicar, B. A. (2015). The cellular mechanisms of neuronal swelling underlying cytotoxic edema. *Cell*, *161*(3), 610–621. https://doi.org/10.1016/j.cell.2015.03.029

Ryuid, V., & Buettner, C. (2019). Fat cells gobbling up norepinephrine? *PLoS Biology*, *17*(2), e3000138. https://doi.org/10.1371/journal.pbio.3000138

Saavedra-Peña, R. M., Taylor, N., Flannery, C., & Rodeheffer, M. S. (2023). Estradiol cycling drives female obesogenic adipocyte hyperplasia. *Cell Reports*, *42*(4), 112390. https://doi.org/10.1016/j.celrep.2023.112390

Sato, M., Horinouchi, T., Hutchinson, D. S., Evans, B. A., & Summers, R. J. (2007). Ligand-directed signaling at the β_3-adrenoceptor produced by 3-(2-ethylphenoxy)-1-[(1,*S*)-1,2,3,4-tetrahydronapth-1-ylamino]-2*S*-2-propanol oxalate (SR59230A) relative to receptor agonists. *Molecular Pharmacology*, *72*(5), 1359–1368. https://doi.org/10.1124/mol.107.035337

Sato, M., Hutchinson, D. S., Evans, B. A., & Summers, R. J. (2008). The β_3-adrenoceptor agonist 4-[[(hexylamino)carbonyl]amino]-*N*-[4-[2-[[(2*S*)-2-hydroxy-3-(4-hydroxyphenoxy)propyl]amino]ethyl]-phenyl]-benzenesulfonamide (L755507) and antagonist (*S*)-*N*-[4-[2-[[3-[3--(acetamidomethyl)phenoxy]-2-hydroxypropyl]amino]-ethyl]phenyl]benzenesulfonamide (L748337) activate different signaling pathways in Chinese hamster ovary-K1 cells stably expressing the human β_3-adrenoceptor. *Molecular Pharmacology*, *74*(5), 1417–1428. https://doi.org/10.1124/mol.108.046979

Schena, G., & Caplan, M. J. (2019). Everything you always wanted to know about β_3-AR * (* but were afraid to ask). *Cells*, *8*(4). https://doi.org/10.3390/cells8040357

Soeder, K. J., Snedden, S. K., Cao, W., Rocca, G. J. D., Daniel, K. W., Luttrell, L. M., & Collins, S. (1999). The β_3-adrenergic receptor activates mitogen-activated protein kinase in adipocytes through a G_i-dependent mechanism. *Journal of Biological Chemistry*, *274*(17), 12017–12022. https://doi.org/10.1074/jbc.274.17.12017

Valentine, J. M., Ahmadian, M., Keinan, O., Abu-Odeh, M., Zhao, P., Zhou, X., Keller, M. P., Gao, H., Yu, R. T., Liddle, C., Downes, M., Zhang, J., Lusis, A. J., Attie, A. D., Evans, R. M., Rydén, M., & Saltiel, A. R. (2022). β_3-Adrenergic receptor downregulation leads to adipocyte catecholamine resistance in obesity. *Journal of Clinical Investigation*, *132*(2). https://doi.org/10.1172/JCI153357

Wang, Y., Leung, V. H., Zhang, Y., Nudell, V. S., Loud, M., Servin-Vences, M. R., Yang, D., Wang, K., Moya-Garzon, M. D., Li, V. L., Long, J. Z., Patapoutian, A., & Ye, L. (2022). The role of somatosensory innervation of adipose tissues. *Nature*, *609*(7927), 569–574. https://doi.org/10.1038/s41586-022-05137-7

Willows, J. W., Blaszkiewicz, M., Lamore, A., Borer, S., Dubois, A. L., Garner, E., Breeding, W. P., Tilbury, K. B., Khalil, A., & Townsend, K. L. (2021). Visualization and analysis of whole depot adipose tissue neural innervation. *IScience*, *24*(10), 103127. https://doi.org/10.1016/j.isci.2021.103127

Wueest, S., Rapold, R. A., Rytka, J. M., Schoenle, E. J., & Konrad, D. (2009). Basal lipolysis, not the degree of insulin resistance, differentiates large from small isolated adipocytes in high-fat fed mice. *Diabetologia*, *52*(3), 541–546. https://doi.org/10.1007/s00125-008-1223-5

Zhai, M., Yang, D., Yi, W., & Sun, W. (2020). Involvement of calcium channels in the regulation of adipogenesis. *Adipocytes*, *9*(1), 132–141. https://doi.org/10.1080/21623945.2020.1738792

Zhang, X. Y., Bi, R. Y., Zhang, P., & Gan, Y. H. (2018). Veratridine modifies the gating of human voltage-gated sodium channel Nav1.7. *Acta Pharmacologica Sinica*, *39*(11), 1716–1724. https://doi.org/10.1038/s41401-018-0065-z

SUPPORTING INFORMATION

Additional supporting information can be found online in the Supporting Information section at the end of this article.

How to cite this article: Goddard, K. E., & Fountain, S. J. (2025). Characterisation of neurogenic lipolytic responses in white adipose tissue ex vivo. *British Journal of Pharmacology*, 1–14. https://doi.org/10.1111/bph.17445